these powers, and also whether the increased Rayleigh range z_R that comes with it still enables efficient transport. This will be the topic of the next section.

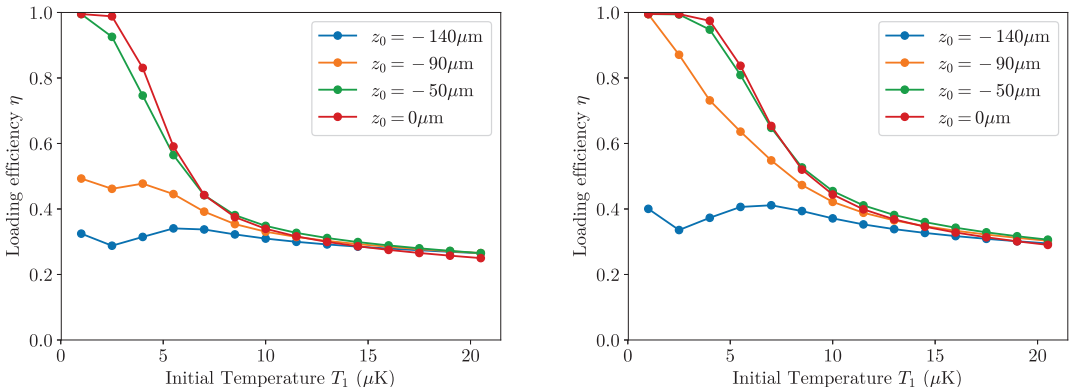

(a) $P_{\text{dipole}} = 4$ W, $I_{\text{coil}} = 27$ A, $w_{y,z} = 50\,\mu$m **(b)** $P_{\text{dipole}} = 8$ W, $I_{\text{coil}} = 27$ A, $w_{y,z} = 70\,\mu$m

Figure 5.15: Transfer efficiency for the whole loading cycle (from magnetic trap into pure dipole trap) in dependence of the initial cloud temperature T_1, for several beam offsets z_0. This takes into account the cloud heating which this process involves. We can observe the dependence on the trap width: For a slightly wider trap (b), the loading efficiency stays large even for higher T_1, but to get the same trap depth we require a more powerful beam. Another interesting observation is that a bigger z_0 favours the small temperature loading rate due to gravity. The connecting lines are guides to the eye.

5.3 Counterdiabatic driving

After the loading of the hybrid trap is completed and the magnetic quadrupole field is switched off, we want to translate the cloud of atoms from the 3D MOT chamber to the science chamber (see fig. 4.1). The distance between those is approximately $d = 400$ mm, although this value has not been finalised yet. In order to achieve this, the focus tunable lenses from section 2.5 will be utilised to axially shift the focus of the dipole beam. As was discussed there, this does not affect its transversal waist, thereby also conserving the Rayleigh range z_{R}, i.e. the axial trap frequency. In the following, we want to find the effect of the translation on the trapping potential and point out how to remedy its effect, assuming the trap is approximated in second order by a harmonic potential of frequency ω. We further assume the transport of a cloud of thermal (uncondensed) atoms at $T \sim 10\,\mu$K. Note that this is only $\sim 8\%$ of the trap depth and hence allows for a classical treatment of this problem.

For the sake of arriving at an adiabaticity condition for the translation, let us consider the case of a trap that is accelerated with a during the first half (for $t < t_f/2$) and $-a$ during the second half of the protocol (for $t > t_f/2$). In such a protocol, the average velocity has half of its maximal value at $t = t_f/2$, i.e. $d/t_f = \bar{v} = v_{\text{max}}/2$. We now require that within an oscillation period $T_{\text{osc}} = 2\pi/\omega$, the trap move over much less than

a Rayleigh range, giving an upper limit for the maximum velocity, $v_{\max} \ll z_{\mathrm{R}}\omega/2\pi$. This translates to an adiabaticity condition for the transport duration $t_f^{\mathrm{ad}} \gg 4\pi d/z_{\mathrm{R}}\omega \approx 30\,\mathrm{s}$ for our set of parameters. In order to keep the experimental cycle time short in favour of obtaining a large dataset to reduce statistical errors, we would like to reduce this value, or increase the transport efficiency for a given transport time t_f, respectively.

In the non-adiabatic velocity regime, the atom cloud experiences a displacement $x_0 \sim z_{\mathrm{R}}$ from the moving trap centre during acceleration[6]. Performing the Galilei transformation into the rest frame of the atom cloud, $x(t) \to x(t) + x_0$, we find for the Hamiltonian

$$H(x + x_0) = \frac{p^2}{2m} + \frac{1}{2}m\omega^2(x + x_0)^2 = \frac{p^2}{2m} + \frac{1}{2}m\omega^2x^2 + m\omega^2x_0x + \frac{1}{2}m\omega^2x_0^2. \tag{5.14}$$

The last term does not depend on x and therefore creates no force, so can be neglected as a mere energy shift. The second but last term then is a pseudo force $F_{\mathrm{p}} = -m\omega^2x_0$ experienced by the atoms during acceleration. This is depicted in fig. 5.16.

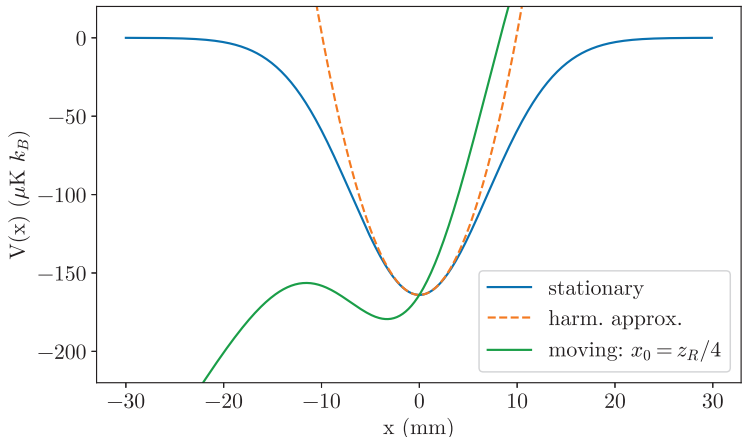

Figure 5.16: Potential for a stationary (blue) and non-adiabatically moving trap (green) in the co-moving frame, where in the latter case the cloud is displaced from the trap centre by $x_0 = z_{\mathrm{R}}/4$. We can observe how the pseudo-force that results from a transport towards positive x skews the Gaussian potential, significantly lowering its depth. For $x_0 \approx z_{\mathrm{R}}/2.5$, the potential has saddle point, i.e. is not confining any more. This is a reproduction of fig. 2 in [Sel18] for our parameters (table 5.1).

The aim of counterdiabatic driving is now to cancel out this pseudo-force, such that the atoms feel a potential that is as close to the pure trap as possible during translation. The differential equation for the driven harmonic oscillator is then

$$m\ddot{q} + F_{\mathrm{p}} = -m\omega^2x, \tag{5.15}$$

[6]For displacements much larger than this, the atom cloud would run out of the potential well and be lost. For the sake of this simple analysis, we assume a constant displacement x_0, i.e. a constant trap acceleration

which gives us the correction to the classical trajectory $q(t)$ in the rest frame that precisely cancels the force acquired in the accelerating frame,

$$\ddot{q} + \omega^2(x - q) = 0, \tag{5.16}$$

such that if we want to drive the trajectory $q(t)$ along x, driving the trajectory

$$q_{\mathrm{CD}}(t) = \ddot{q}(t)/\omega^2 + q(t) \tag{5.17}$$

instead ensures that – provided we have a deep enough potential – the motion-induced pseudo force gets compensated. This is the equivalent of a waiter tipping his tray when accelerating the glasses on it, and tipping it the opposite way when decelerating. A more in-depth derivation of this protocol can be found in section A.1.5.

In order for the eigenstates of the classical and counterdiabatic Hamiltonian to match up at $t = 0$ and $t = t_f$ (cf. section A.1.5), we set the following boundary conditions:

$$\begin{aligned} q(0) = 0, \dot{q}(0) = 0, \ddot{q}(0) = 0 \\ q(t_f) = d, \dot{q}(t_f) = 0, \ddot{q}(t_f) = 0 \end{aligned} \tag{5.18}$$

These are satistified e.g. by the polynomial [Tor11]

$$q(t) = d\left(10\left(\frac{t}{t_f}\right)^3 - 15\left(\frac{t}{t_f}\right)^4 + 6\left(\frac{t}{t_f}\right)^5\right) \tag{5.19}$$

The limitation of a deep enough potential stated before can be expressed in more quantitative terms: The counterdiabatic protocol works by adjusting the trap trajectory such that this shift cancels out the effects of the pseudo-force over the duration of the protocol. The maximum accelerating force $F = -\mathrm{grad}\, U_{\mathrm{dipole}} = ma$ that can be exerted by the dipole beam is to be found at the point of its maximum absolute slope, and has the value

$$F_{\max} = U_0 \frac{1}{w_0\sqrt{e}} \tag{5.20}$$

where $w_0 = \sqrt{\frac{2U_0}{m\omega^2}}$ is the beam waist. Plugging this into eq. 5.20 gives us the maximum possible acceleration for our set of beam parameters discussed in section 5.1:

$$a_{\max} = F_{\max}/m = \sqrt{\frac{U_0\omega^2}{2me}} \approx 1.3\,\frac{\mathrm{m}}{\mathrm{s}^2}. \tag{5.21}$$

The trajectory from eq. 5.19 has a maximum acceleration of

$$\ddot{q}_{\max} = \frac{10d}{t_f^2\sqrt{3}}. \tag{5.22}$$

Equating 5.22 and 5.21 gives us a lower limit for the counterdiabatic transport time: $t_f^{\mathrm{CD}} = 1.30\,\mathrm{s}$. Figure 5.17 shows the trajectory (equation 5.17) which moves our trap about our desired value d in this minimum transport time.

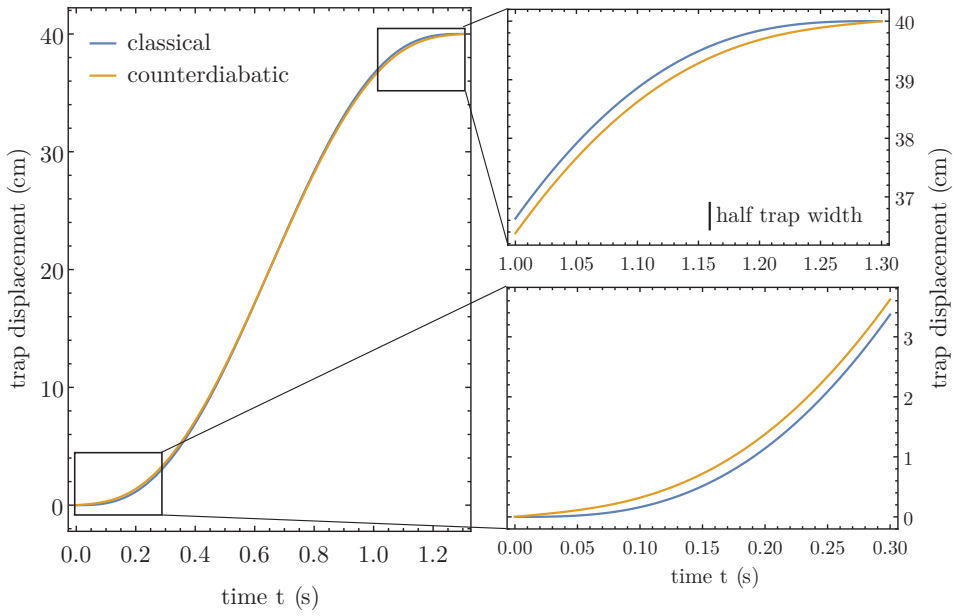

Figure 5.17: Counterdiabatic correction to the classical trajectory (equation 5.19). We see that these happen on the length scale of half the trap width (Rayleigh range).

The datasheet of the focus-tunable lenses[7] quotes a focus reprodicibility of $\Delta P = \pm 0.05$ dioptres using the factory driver. If we assume a collimated beam before the tunable lens as depicted in fig. 2.14, this translates to a focal length instability of $\Delta f = \Delta P / P^2 \approx 8\,\mathrm{mm}$, which is slightly smaller than the Rayleigh range of the dipole beam. Ideally, we would like to have a focus reproducibility of $\sim 1\,\mathrm{mm}$, which could be met either by reducing the optical power P which the tunable lens is supposed to provide, i.e. pre-focusing the beam, or by devising a custom software driver for the lens, including an active feedback for the focal length which is not implemented in the factory driver. A control algorithm could take the signal of a photodiode behind a pinhole as an error signal to instantaneously control the focus position.

5.3.1 Truncated Wigner Approach

In order to design the trap trajectory further, it would be desirable to have a measure of the heating or the state transfers that happen during transport, depending on the choice of t_f relative to t_f^{ad} and t_f^{CD}, the trap depth and its waist. For this purpose, a numerical simulation of specific transport trajectories would be helpful.

As was discussed in the last section, the fact that five orders of magnitude lie between the harmonic oscillator length $\sqrt{\hbar/m\omega} = 5.6\,\mu\mathrm{m}$ and the final trap displacement, as well as the system's significant temperature make a full quantum-mechanical simulation

[7] Optotune EL-16-40-TC-NIR-5D

numerically intractable. While we could show the principle to work for distances of several hundred harmonic oscillator lengths[8], its extension required either an unfeasible amount of time steps or of spatial points, depending on the choice of simulation units. As we work with an uncondensed atom cloud, however, a fully coherent simulation is not even necessary, as we will quantify in the next section.

In order to simulate the trap dynamics, a semiclassical approach starting from the *Wigner function* $W(p,q)$ [Wig32] was chosen. It is the quantum mechanical equivalent to the phase space density function of a classical system,

$$W(p,q) = \int d\xi \, \langle q - \xi/2 | \, \hat{\rho} \, | q + \xi/2 \rangle \exp(ip\xi/\hbar), \tag{5.23}$$

where ρ describes the density operator of the quantum system, and is frequently used to describe dynamics in Bose–Einstein condensates without solving the full Gross–Pitaevskii equation[Ste98]. Since our envisioned trap depth is much higher than the cloud temperature of a few μK, we can approximate it by a harmonic potential. As is derived in [Pol10], for a harmonic oscillator and its thermal density matrix,

$$\mathcal{H} = \frac{p^2}{2m} + \frac{m\omega^2}{2}q^2, \qquad \hat{\rho} = \frac{1}{Z}\sum_n \exp(-\frac{\hbar\omega}{k_B T}) \, |n\rangle \langle n| \tag{5.24}$$

with $|n\rangle$ the harmonic oscillator eigenstates, it can be shown that

$$W(p,q,T) \propto \frac{\hbar\omega}{T} \exp\left(-\beta_{\text{eff}}\left(\frac{p^2}{2m} + \frac{m\omega^2}{2}q^2\right)\right) \quad \text{where } \beta_{\text{eff}} = \frac{2}{\hbar\omega}\tanh(\beta\hbar\omega/2), \tag{5.25}$$

and $\beta \equiv 1/k_B T$. We can see that for $T \to \infty$, $\beta_{\text{eff}} \to \beta$ and we retrieve the classical Boltzmann distribution from eq. 5.6. We can therefore see β_{eff} as the result of a quantum correction, and since in our case $(\beta_{\text{eff}} - \beta)/\beta \sim 10^{-9}$, these become relevant only on large time scales.

Following the approach taken by [Ste98], we therefore use a semiclassical approach here: we randomly sample initial positions and momenta of single particles according to the density function (equation 5.25) and subsequently evolve them under Newton's classical equations, where we assume that they are in an essentially non-interacting regime. This is called the *truncated Wigner approximation* (TWA). As suggested by Sels [Sel], the state evolution can be performed using the efficient *Verlet algorithm* which is an implementation of the well-known leap frog integration technique for Newton's equations:

$$\begin{aligned}
x(t+\Delta t) &= x(t) + \frac{\Delta t}{2}p(t), \\
p(t+\Delta t) &= p(t) + \frac{\ddot{x}(t) + \ddot{x}(t+\Delta t)}{2m} = p(t) - \Delta t(x(t) - q(t))\frac{U_0}{m}\exp\left(-(x(t)-q(t))^2/2z_R^2\right), \\
x(t+\Delta t) &= x(t) + \frac{\Delta t}{2}p(t)
\end{aligned} \tag{5.26}$$

[8] using both a discretising PDE integrator and a split-step Fourier method

where we used the definition of our moving Gaussian trap potential[9]. In order to keep numerical constants small, the simulation is performed with energy in units of trap depth, x in units of z_R, mass in units of m_{Rb} and time in units of the inverse trap frequency.

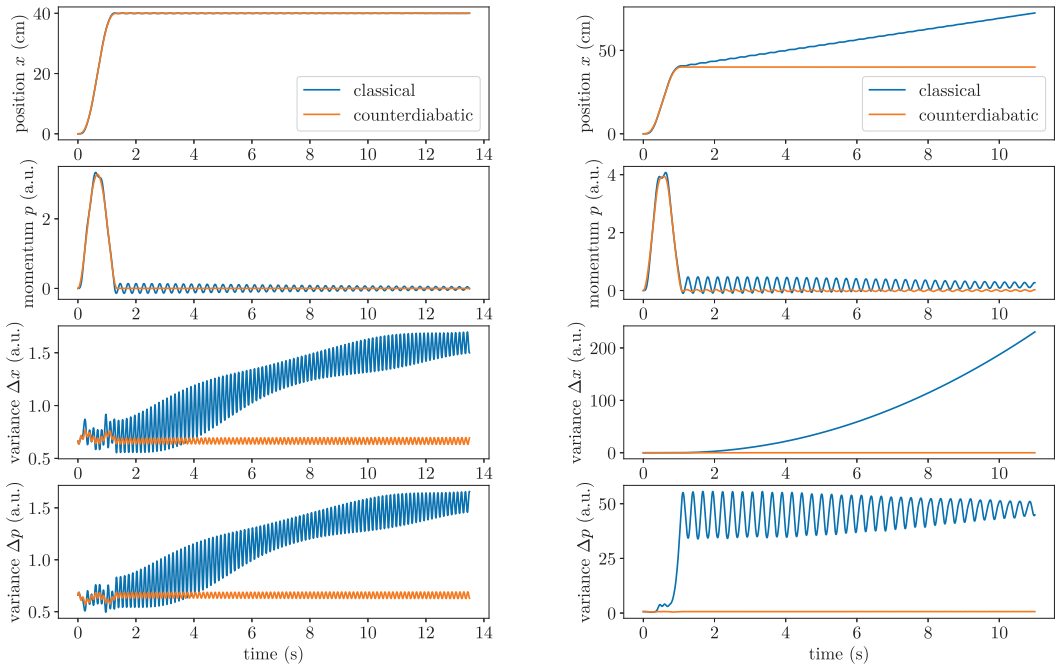

(a) $t_f = 1.35\,\mathrm{s}$. **(b)** $t_f = 1.1\,\mathrm{s}$.

Figure 5.18: Truncated Wigner simulations for $d = 400\,\mathrm{mm}$, $T = 2\,\mu\mathrm{K}$ and all other parameters from table 5.1. The trajectory from eq. 5.19 and its counterdiabatic correction according to eq. 5.17 were simulated. For small t_f (b), the cloud runs out of the trap after deceleration with the classical trajectory, whereas the counterdiabatic correction manages to "catch" it.

Figure 5.18 clearly shows the positive effect of the counterdiabatic trajectory on the performance of the trap, as it reduces fluctuations in both momentum and position. In panel (b), it can be seen that the counterdiabatic protocol even manages to keep the atom cloud trapped for transport velocities where the maximum deceleration in the classical protocol would not be enough to contain the cloud within the trap, i.e. it would run out.

In order to arrive at a measure for the heating during transport, we use the temperature dependence of the Wigner function to map the width of the steady state Wigner function after transport (after $\sim 10t_f$) to a relative temperature increase. This is shown in fig. 5.19, where we observe that due to our rather deep trap, the counterdiabatic protocol ensures essentially heatingless transport down to our calculated t_f^{CD}, whereas the classical

[9] For small $T \ll U_0/k_B$, this reduces to a harmonic potential as used in eq. 5.24. For higher temperatures, it captures the flat background of our potential which is crucial to fig. 5.18.

trajectory shows strong heating in this regime. As we would expect, the heating rate of the latter shows fluctuations at the trapping frequency ω.

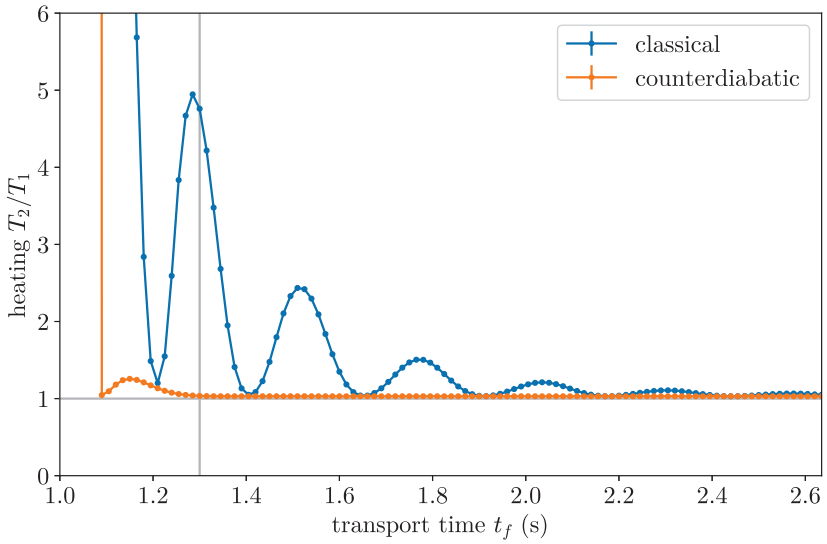

Figure 5.19: Truncated Wigner simulation of the trap trajectory from fig. 5.18 in dependence of the transport time t_f. Both the classical and counterdiabatic trajectory shoot off to $\sim 10^5\,\mathrm{K}$ for $t_f \approx 1\,\mathrm{s}$. The grey vertical line at $t = t_f^{\mathrm{CD}}$ shows that our calculation matches the simulation, although there seems to be another point at $t \approx 1.1\,\mathrm{s} < t_f^{\mathrm{CD}}$ for which we achieve transport without significant heating.

These simulations show the effect of counterdiabatically translating the dipole trap between the two chambers and conclude the design of the hybrid trapping system.

A.1.5 Counterdiabatic driving

This section derives the protocol for a counterdiabatic translation (equation 5.17), roughly following the argumentation in [Sel17].

Suppose $|\Psi\rangle$ is our wavefunction in the rest frame, and is connected to the moving frame wavefunction $|\tilde{\Psi}\rangle$ via a unitary transformation $U(\lambda)$ as $|\Psi\rangle = U(\lambda)|\tilde{\Psi}\rangle$. In the moving frame, the Schrödinger equation becomes

$$\begin{aligned} i\hbar\frac{d(U(\lambda)|\tilde{\Psi}\rangle)}{dt} &= \mathcal{H}U(\lambda)|\tilde{\Psi}\rangle \\ i\hbar\frac{dU(\lambda)}{dt}|\tilde{\Psi}\rangle + i\hbar U(\lambda)\frac{d|\tilde{\Psi}\rangle}{dt} &= \mathcal{H}(U(\lambda)|\tilde{\Psi}\rangle) \end{aligned} \tag{A.5.26}$$

for the trap Hamiltonian $\mathcal{H}$. Multiplying by $U^\dagger(\lambda)$ from the left gives

$$i\hbar U^\dagger(\lambda)\frac{dU(\lambda)}{dt}|\tilde{\Psi}\rangle + i\hbar\underbrace{U^\dagger(\lambda)U(\lambda)}_{=1}\frac{d|\tilde{\Psi}\rangle}{dt} = \underbrace{U^\dagger(\lambda)\mathcal{H}U(\lambda)}_{=\tilde{\mathcal{H}}}|\tilde{\Psi}\rangle \tag{A.5.27}$$

where we recognise $U^\dagger\mathcal{H}U$ as the transformation of the Hamiltonian into the moving frame. Expressing the time derivative on the left hand side by a chain rule, $\frac{d}{dt} = \frac{\partial\lambda}{\partial t}\frac{\partial}{\partial\lambda} \equiv \dot{\lambda}\partial_\lambda$, we can rewrite the first term in equation A.5.27 as

$$\dot{\lambda}\underbrace{U^\dagger(\lambda)\,(i\hbar\partial_\lambda)\,U(\lambda)}_{\tilde{A}_\lambda}|\tilde{\Psi}\rangle \tag{A.5.28}$$

such that equation A.5.27 becomes

$$i\hbar\frac{d|\tilde{\Psi}\rangle}{dt} = \left(\tilde{\mathcal{H}} - \dot{\lambda}\tilde{A}_\lambda\right)|\tilde{\Psi}\rangle. \tag{A.5.29}$$

$A_\lambda \equiv i\hbar\partial_\lambda$ is often called a *gauge potential* since by its nature of a derivation operator it has no effect on the equations of motion[10] in the moving frame, but can however induce non-adiabatic transitions between energy levels. If we identify $U(\lambda)$ with a spatial translation $x \to x - \lambda(t)$, we see that $A_\lambda = i\hbar\frac{d}{dx}$ becomes the momentum operator $\hat{p}$.[11] The task is now to recover the original Hamiltonian $\mathcal{H}$ in the moving frame by adjusting $\mathcal{H} \to \mathcal{H}_{\mathrm{CD}}$, which we call the *counterdiabatic Hamiltonian*. Naively, one would assume that setting

$$\mathcal{H}_{\mathrm{CD}} = \mathcal{H} + \dot{\lambda}\tilde{A}_\lambda \tag{A.5.31}$$

[10] In the Hamilton formalism, for a time-dependent Hamiltonian $\mathcal{H}$, these are given by

$$\dot{\mathbf{p}} = -\frac{\partial\mathcal{H}}{\partial q}, \quad \dot{\mathbf{q}} = \frac{\partial\mathcal{H}}{\partial p}. \tag{A.5.30}$$

[11] In this case, we can even see an analogy to classical electrodynamics where the Lagrange function becomes $\mathcal{L} = T - V = \frac{1}{2}mv^2 + \frac{e}{c}\mathbf{v}\cdot\mathbf{A} - e\phi$, where $\mathbf{A}$ is the gauge-dependent vector potential.

in the rest frame would do the job, so as to counteract the contribution in equation A.5.29. We can verify that this is indeed the case by doing the above derivation in reverse, e.g. considering the effect of the rest frame Hamiltonian $\mathcal{H} + \dot{\lambda}A_\lambda$ in the moving frame:

$$\begin{aligned} i\hbar\frac{d\left|\Psi\right\rangle}{dt} &= \left(\mathcal{H} + \dot{\lambda}A_\lambda\right)\left|\Psi\right\rangle \\ i\hbar\frac{d}{dt}\left(U(\lambda)\left|\tilde{\Psi}\right\rangle\right) &= \left(\mathcal{H} + \dot{\lambda}A_\lambda\right)U(\lambda)\left|\Psi\right\rangle \\ i\hbar\underbrace{\frac{dU}{dt}}_{=\dot{\lambda}\partial_\lambda U}\left|\tilde{\Psi}\right\rangle + i\hbar U\frac{d\left|\tilde{\Psi}\right\rangle}{dt} &= \mathcal{H}U(\lambda)\left|\tilde{\Psi}\right\rangle + \dot{\lambda}A_\lambda U(\lambda)\left|\tilde{\Psi}\right\rangle \\ \underbrace{U^\dagger\left(i\hbar\dot{\lambda}\partial_\lambda\right)U}_{=\tilde{A_\lambda}}\left|\tilde{\Psi}\right\rangle + i\hbar\frac{d\left|\tilde{\Psi}\right\rangle}{dt} &= \underbrace{U^\dagger\mathcal{H}U}_{\tilde{\mathcal{H}}}\left|\tilde{\Psi}\right\rangle + \underbrace{U^\dagger\dot{\lambda}A_\lambda U}_{=\tilde{A_\lambda}}\left|=\tilde{\Psi}\right\rangle \\ i\hbar\frac{d\left|\tilde{\Psi}\right\rangle}{dt} &= \tilde{\mathcal{H}}\tilde{A_\lambda}, \end{aligned} \tag{A.5.32}$$

i.e. the time evolution in the moving frame is now free from non-adiabatic transitions since $\tilde{\mathcal{H}}$ is designed to be diagonal. This verifies equation A.5.31, from which we can also see that $\mathcal{H}_{\mathrm{CD}}$ coincides with $\mathcal{H}$ in the case of zero velocity $\dot{\lambda} = 0$, which means that in order to transport from and to eigenstates of $\mathcal{H}$, the protocol has to start and end with zero velocity, as implemented in equation 5.18.

Considering the experimental case in the approximation of a harmonic oscillator, we have $\mathcal{H} = \frac{p^2}{2m} + V\left(q - \lambda(t)\right), V(q) = \frac{m\omega^2}{2}q^2$ for the conjugate variables of position q and momentum p, and $\lambda(t)$ a displacement in space. Now the Hamiltonian from equation A.5.31 which couples directly to the momentum operator is experimentally rather hard to realise. We therefore employ a gauge transformation [12] $p \to p - m\dot{\lambda}, V \to V - m\ddot{\lambda}q$, giving

$$\mathcal{H}_{\mathrm{CD}} = \frac{p^2}{2m} - \dot{\lambda}p + \dot{\lambda}p + \frac{m\dot{\lambda}^2}{2} + \frac{m\omega^2}{2}\left(q - \lambda(t)\right)^2 - m\ddot{\lambda}q. \tag{A.5.33}$$

As we can see in equation A.5.30, terms that do not explicitly depend on p or q do not contribute to the equations of motion and can be neglected. The challenge is then to engineer the rightmost term in the above equation. However, when we complete the square of the last two terms and again omit the parts without explicit p or q dependence, we find that the counterdiabatic Hamiltonian is equivalent to

$$\mathcal{H}_{\mathrm{CD}} = \frac{p^2}{2m} + \frac{m\omega^2}{2}\left(q - \lambda(t) - \frac{\ddot{\lambda}}{\omega^2}\right)^2. \tag{A.5.34}$$

This amounts just to an additional displacement $\ddot{\lambda}/\omega^2$, as in equation 5.17.

[12] Again, this is similar to classical electrodynamics where the equations of motion are $\mathbf{E} = -\boldsymbol{\nabla}V - \frac{\partial\mathbf{A}}{\partial t}, \mathbf{B} = \boldsymbol{\nabla}\times\mathbf{A}$ for the scalar and vector potentials V and $\mathbf{A}$, respectively. A gauge transformation then means $\mathbf{A} \to \mathbf{A} + \boldsymbol{\nabla}f, V \to V - \frac{\partial f}{\partial t}$ for an arbitrary $f(x,t)$, since $\boldsymbol{\nabla}\times(\boldsymbol{\nabla}f) = 0$. In the case described in the text, $f(q,p) = -m\dot{\lambda}q$ and we identify the vector potential $\mathbf{A}$ with the momentum p, as derived above.

Bibliography

[Alb15] A. Alberti *et al.*, *Super-resolution microscopy of single atoms in optical lattices.* New Journal of Physics **18**, 053010 (2015) (cit. on p. 27).

[And73] P. W. Anderson, *Resonating valence bonds: A new kind of insulator?* Materials Research Bulletin **8**, 153 (1973) (cit. on p. 6).

[And95] M. H. Anderson *et al.*, *Observation of Bose-Einstein Condensation in a Dilute Atomic Vapor.* Science **269**, 198 (1995) (cit. on p. 3).

[Bak09] W. S. Bakr *et al.*, *A quantum gas microscope for detecting single atoms in a Hubbard-regime optical lattice.* Nature **462**, 74 (2009) (cit. on p. 4).

[Bal10] L. Balents, *Spin liquids in frustrated magnets.* Nature **464**, 199 (2010) (cit. on p. 5).

[Bol16] M. Boll *et al.*, *Spin- and density-resolved microscopy of antiferromagnetic correlations in Fermi-Hubbard chains.* Science **353**, 1257 (2016) (cit. on p. 8).

[Bra13] S. Braun *et al.*, *Negative absolute temperature for motional degrees of freedom.* Science **339**, 52 (2013) (cit. on pp. 9, 32).

[Bra15] C. Braun, *Implementation of a Raman Sideband Cooling for 87Rb.* B.Sc. thesis. Universität Stuttgart, 2015 (cit. on p. 16).

[Bur97] E. A. Burt *et al.*, *Coherence, correlations, and collisions: What one learns about Bose-Einstein condensates from their decay.* Physical Review Letters **79**, 337 (1997) (cit. on pp. 51, 52).

[Cat06] J. Catani *et al.*, *Intense slow beams of bosonic potassium isotopes.* Physical Review A - Atomic, Molecular, and Optical Physics **73**, 033415 (2006) (cit. on p. 36).

[Che14] D. Chen, *Anti-Helmholtz magnetic trap Electromagnetism review*. 2014. URL: http://publish.illinois.edu/davidchen/files/2012/10/Anti-Helmholtz-magnetic-trap.pdf (cit. on p. 17).

[Che15] L. W. Cheuk *et al.*, *Quantum-Gas Microscope for Fermionic Atoms*. Physical Review Letters **114**, 193001 (2015) (cit. on p. 4).

[Chi10] C. Chin *et al.*, *Feshbach resonances in ultracold gases*. Reviews of Modern Physics **82**, 1225 (2010) (cit. on p. 32).

[Cle76] C. L. Cleveland and R. Medina A., *Obtaining a Heisenberg Hamiltonian from the Hubbard model*. American Journal of Physics **44**, 44 (1976) (cit. on p. 5).

[Coh90] C. N. Cohen-Tannoudji and W. D. Phillips, *New Mechanisms for Laser Cooling*. Physics Today **43**, 33 (1990) (cit. on p. 13).

[Dav95] K. B. Davis *et al.*, *Observation of Bose-Einstein condensation in a gas of sodium Vapor*. Physical Review Letters **75**, 3969 (1995) (cit. on p. 3).

[De 09] M. A. De Vries *et al.*, *Scale-Free Antiferromagnetic Fluctuations in the s=1/2 Kagome Antiferromagnet Herbertsmithite*. Physical Review Letters **103**, 237201 (2009) (cit. on p. 32).

[DeM99] B. DeMarco and D. S. Jin, *Onset of Fermi Degeneracy in a Trapped Atomic Gas*. Science **285**, 1703 (1999) (cit. on p. 3).

[Don99] X. Dong *et al.*, *Current-induced guiding and beam steering in active semiconductor planar waveguide*. IEEE Photonics Technology Letters **11**, 809 (1999) (cit. on p. 47).

[Duf10] G. Dufour, *Etude des collisions entre atomes froids de rubidium et un gaz chaud*. Research report. University of British Columbia, Vancouver, 2010 (cit. on p. 34).

[Ear42] S. Earnshaw, *On the Nature of the Molecular Forces which Regulate the Constitution of the Luminiferous Ether*. Trans. Camb. Phil. Soc. **7**, 97 (1842) (cit. on p. 17).

[Edg15] G. J. Edge *et al.*, *Imaging and addressing of individual fermionic atoms in an optical lattice*. Physical Review A - Atomic, Molecular, and Optical Physics **92**, 063406 (2015) (cit. on p. 4).

[Esc03] J. Eschner *et al.*, *Laser cooling of trapped ions*. Journal of the Optical Society of America B **20**, 1003 (2003) (cit. on p. 16).

[Fey82] R. P. Feynman, *Simulating Physics with computers*. International Journal of Theoretical Physics **21**, 467 (1982) (cit. on p. 1).

[Foo05] C. J. Foot, *Atomic Physics*. Oxford University Press, USA (2005) (cit. on pp. 11, 13, 17, 19).

[Fre94] J. K. Freericks and H. Monien, *Phase diagram of the Bose-Hubbard Model*. Europhysics Letters **26**, 545 (1994) (cit. on p. 2).

[Fuh12] A. Fuhrmanek *et al.*, *Light-assisted collisions between a few cold atoms in a microscopic dipole trap*. Physical Review A - Atomic, Molecular, and Optical Physics **85**, 062708 (2012) (cit. on p. 23).

[Gre02] M. Greiner *et al.*, *Quantum phase transition from a superfluid to a mott insulator in a gas of ultracold atoms*. Nature **415**, 39 (2002) (cit. on pp. 3, 6).

[Gri00] R. Grimm, M. Weidemüller, and Y. B. Ovchinnikov, *Optical Dipole Traps for Neutral Atoms*. Advances in Atomic, Molecular and Optical Physics **42**, 95 (2000) (cit. on pp. 19, 20).

[Hal15] E. Haller *et al.*, *Single-atom imaging of fermions in a quantum-gas microscope*. Nature Physics **11**, 738 (2015) (cit. on p. 4).

[Han12] T. H. Han *et al.*, *Fractionalized excitations in the spin-liquid state of a kagome-lattice antiferromagnet*. Nature **492**, 406 (2012) (cit. on p. 9).

[Ism16] N. Ismail *et al.*, *Fabry-Pérot resonator: spectral line shapes, generic and related Airy distributions, linewidths, finesses, and performance at low or frequency-dependent reflectivity*. Optics Express **24**, 16366 (2016) (cit. on p. 43).

[Jak98] D. Jaksch *et al.*, *Cold bosonic atoms in optical lattices*. Physical Review Letters **81**, 3108 (1998) (cit. on p. 2).

[Jo12] G.-B. Jo *et al.*, *Ultracold Atoms in a Tunable Optical Kagome Lattice*. Physical Review Letters **108**, 045305 (2012) (cit. on p. 9).

[Jör08] R. Jördens *et al.*, *A Mott insulator of fermionic atoms in an optical lattice*. Nature **455**, 204 (2008) (cit. on p. 3).

[Kas92] M. Kasevich and S. Chu, *Laser cooling below a photon recoil with three-level atoms*. Physical Review Letters **69**, 1741 (1992) (cit. on p. 16).

[Ket99] W. Ketterle, D. S. Durfee, and D. M. Stamper-Kurn, *Making, probing and understanding Bose-Einstein condensates*. arXiv:9904034v2 (1999). URL: `http://arxiv.org/abs/cond-mat/9904034` (cit. on p. 18).

[Kno12] S. Knoop *et al.*, *Nonexponential one-body loss in a Bose-Einstein condensate*. Physical Review A - Atomic, Molecular, and Optical Physics **85**, 025602 (2012) (cit. on pp. 34, 52).

[Lee06] P. A. Lee, N. Nagaosa, and X. G. Wen, *Doping a Mott insulator: Physics of high-temperature superconductivity*. Reviews of Modern Physics **78**, 17 (2006) (cit. on pp. 3, 5).

[Léo14] J. Léonard *et al.*, *Optical transport and manipulation of an ultracold atomic cloud using focus-tunable lenses*. New Journal of Physics **16**, 093028 (2014) (cit. on p. 22).

[Lia17] H. J. Liao *et al.*, *Gapless Spin-Liquid Ground State in the S=1 /2 Kagome Antiferromagnet*. Physical Review Letters **118**, 1 (2017) (cit. on pp. 9, 32).

[Lin09] Y. J. Lin *et al.*, *Rapid production of R 87 b Bose-Einstein condensates in a combined magnetic and optical potential*. Physical Review A - Atomic, Molecular, and Optical Physics **79**, 063631 (2009) (cit. on p. 21).

[Loh90] E. Y. Loh *et al.*, *Sign problem in the numerical simulation of many-electron systems*. Physical Review B **41**, 9301 (1990) (cit. on p. 32).

[Maj32] E. Majorana, *Atomi orientati in campo magnetico variabile*. Nuovo Cimento **9**, 43 (1932) (cit. on p. 18).

[Maz17] A. Mazurenko *et al.*, *A cold-atom Fermi-Hubbard antiferromagnet*. Nature **545**, 462 (2017) (cit. on pp. 5, 8).

[Mel] M. Melchner, *private communication* (cit. on p. 36).

[Mel17] M. Melchner, *An optical dipole trap for ultracold atomic gases*. M.Sc. thesis. University of Cambridge, 2017 (cit. on pp. 57, 80).

[Men08] C. Menotti and N. Trivedi, *Spectral weight redistribution in strongly correlated bosons in optical lattices*. Physical Review B - Condensed Matter and Materials Physics **77**, 235120 (2008) (cit. on p. 2).

[Men10] Z. Y. Meng *et al.*, *Quantum spin liquid emerging in two-dimensional correlated Dirac fermions*. Nature **464**, 847 (2010) (cit. on p. 9).

[Met99] H. J. Metcalf and P. van der Straten, *Laser Cooling and Trapping 1*, 1 (1999) (cit. on p. 13).

[Mir15] M. Miranda *et al.*, *Site-resolved imaging of ytterbium atoms in a two-dimensional optical lattice*. Physical Review A - Atomic, Molecular, and Optical Physics **91**, 1 (2015) (cit. on p. 4).

[Mit18] D. Mitra *et al.*, *Quantum gas microscopy of an attractive Fermi-Hubbard system*. Nature Physics **14**, 173 (2018) (cit. on pp. 4, 8, 28).

[Mod01] G. Modugno *et al.*, *Bose-Einstein condensation of potassium atoms by sympathetic cooling*. Science **294**, 1320 (2001) (cit. on p. 23).

[Nes08] J. Nes, *Cold Atoms and Bose-Einstein Condensates in Optical Dipole Potentials*. PhD thesis. Technische Universität Darmstadt, 2008 (cit. on p. 51).

[Omr15] A. Omran *et al.*, *Microscopic Observation of Pauli Blocking in Degenerate Fermionic Lattice Gases*. Physical Review Letters **115**, 263001 (2015) (cit. on p. 4).

[Par15] M. F. Parsons *et al.*, *Site-Resolved Imaging of Fermionic Li-6 in an Optical Lattice*. Physical Review Letters **114**, 213002 (2015) (cit. on p. 4).

[Pet95] W. Petrich *et al.*, *Stable, tightly confining magnetic trap for evaporative cooling of neutral atoms*. Physical Review Letters **74**, 3352 (1995) (cit. on p. 21).

[Pol10] A. Polkovnikov, *Phase space representation of quantum dynamics*. Annals of Physics **325**, 1790 (2010) (cit. on p. 65).

[Pri83] D. E. Pritchard, *Cooling neutral atoms in a magnetic trap for precision spectroscopy*. Physical Review Letters **51**, 1336 (1983) (cit. on p. 21).

[Sch10] U. Schneider, *Interacting Fermionic Atoms in Optical Lattices—A Quantum Simulator for Condensed Matter Physics*. PhD thesis. Universität Mainz, 2010. URL: `http://ubm.opus.hbz-nrw.de/volltexte/2011/2860/` (cit. on p. 4).

[Sel] D. Sels, *private communication* (cit. on p. 65).

[Sel17] D. Sels and A. Polkovnikov, *Minimizing irreversible losses in quantum systems by local counter-diabatic driving*. Proceedings of the National Academy of Sciences of the United States of America **114**, 3909 (2017) (cit. on p. 82).

[Sel18] D. Sels, *Stochastic gradient ascent outperforms gamers in the Quantum Moves game*. Physical Review A **97**, 040302 (2018) (cit. on pp. 10, 62).

[She10] J. F. Sherson *et al.*, *Single-atom-resolved fluorescence imaging of an atomic Mott insulator*. Nature **467**, 68 (2010) (cit. on p. 4).

[Sie86] A. E. Siegman, *Lasers*. University Science Books, 1986, 2. ISBN: 0935702113 (cit. on pp. 41, 42).

[Sim11] J. Simon *et al.*, *Quantum simulation of antiferromagnetic spin chains in an optical lattice*. Nature **472**, 307 (2011) (cit. on pp. 6, 7).

[Ste] D. A. Steck, *Rubidium 87 D Line Data*. URL: `http://steck.us/alkalidata` (cit. on pp. 13, 79).

[Ste98] M. J. Steel *et al.*, *Dynamical quantum noise in trapped Bose-Einstein condensates*. Phys. Rev. A **58**, 4824 (1998) (cit. on p. 65).

[Stö16] F. M. Störtz, *Towards quantum simulation with ultracold molecules*. B.Sc. thesis. University of Heidelberg, 2016 (cit. on p. 12).

[Suk97] C. V. Sukumar and D. M. Brink, *Spin-flip transitions in a magnetic trap*. Physical Review A **56**, 2451 (1997) (cit. on p. 18).

[Tho17] C. K. Thomas, *Quantum Simulation of Triangular, Honeycomb and Kagome Crystal Structures using Ultracold Atoms in Lattices of Laser Light*. PhD thesis. University of California, Berkeley, 2017 (cit. on pp. 26, 30).

[Tie11] T. G. Tiecke, *Properties of Potassium*. 2011. URL: `http://www.tobiastiecke.nl/archive/PotassiumProperties.pdf` (cit. on p. 14).

[Tor11] E. Torrontegui *et al.*, *Fast atomic transport without vibrational heating*. Physical Review A - Atomic, Molecular, and Optical Physics **83**, 013415 (2011) (cit. on p. 63).

[Tro08] S. Trotzky *et al.*, *Time-resolved observation and control of superexchange interactions with ultracold atoms in optical lattices*. Science **319**, 295 (2008) (cit. on pp. 7, 8).

[Ver04] F. Verstraete and J. I. Cirac, *Renormalization algorithms for Quantum-Many Body Systems in two and higher dimensions*. arXiv:0407066 (2004). URL: `https://arxiv.org/abs/cond-mat/0407066` (cit. on p. 9).

[Vie18] K. Viebahn *et al.*, *Matter-wave diffraction from a quasicrystalline optical lattice*. arXiv:1807.00823v1 (2018). URL: `https://arxiv.org/pdf/1807.00823.pdf` (cit. on pp. 22, 35, 41).

[Wan50] G. H. Wannier, *Antiferromagnetism. The triangular Ising net*. Physical Review **79**, 357 (1950) (cit. on pp. 5, 32).

[Web03] T. Weber *et al.*, *Three-body recombination at large scattering lengths in an ultracold atomic gas*. Physical Review Letters **91**, 123201 (2003) (cit. on p. 51).

[Wei03] M. Weidemüller and C. Zimmermann, eds., *Interactions in Ultracold Gases: From atoms to molecules*. Wiley VCH, 2003. ISBN: 3527635076 (cit. on p. 2).

[Wei09] M. Weidemüller and C. Zimmermann, eds., *Cold Atoms and Molecules*. Wiley VCH, 2009 (cit. on p. 51).

[Wei11] C. Weitenberg *et al.*, *Single-spin addressing in an atomic Mott insulator*. Nature **471**, 319 (2011) (cit. on p. 5).

[Wei17] C. H. Wei and S. H. Yan, *Raman sideband cooling of rubidium atoms in optical lattice*. Chinese Physics B **26**, 080701 (2017) (cit. on p. 16).

[Wig32] E. Wigner, *On the quantum correction for thermodynamic equilibrium*. Physical Review **40**, 749 (1932) (cit. on p. 65).

[Wil08] R. A. Williams *et al.*, *Dynamic optical lattices: two-dimensional rotating and accordion lattices for ultracold atoms*. Optics Express **16**, 16977 (2008) (cit. on p. 28).

[Wis01] E. Wiseman, *Degenerate fermion gas heating by hole creation*. Physical Review Letters **87**, 240403 (2001) (cit. on p. 23).

[Yam16] R. Yamamoto *et al.*, *An ytterbium quantum gas microscope with narrow-line laser cooling*. New Journal of Physics **18**, 023016 (2016) (cit. on p. 4).

[Yan11] S. Yan, D. A. Huse, and S. R. White, *Spin-Liquid Ground State of the S=1/2 Kagome Heisenberg Antiferromagnet*. Science **332**, 1173 (2011) (cit. on p. 9).